

## Theory of Single-Spin Inelastic Tunneling Spectroscopy

J. Fernández-Rossier

*Departamento de Física Aplicada, Universidad de Alicante, San Vicente del Raspeig, 03690 Spain*

(Received 19 January 2009; published 23 June 2009)

I show that recent experiments of inelastic scanning tunneling spectroscopy of single and a few magnetic atoms are modeled with a phenomenological spin-assisted tunneling Hamiltonian so that the inelastic  $dI/dV$  line shape is related to the spin spectral weight of the magnetic atom. This accounts for the spin selection rules and  $dI/dV$  spectra observed experimentally for single Fe and Mn atoms deposited on  $\text{Cu}_2\text{N}$ . In the case of chains of Mn atoms it is found necessary to include both first and second-neighbor exchange interactions as well as single-ion anisotropy.

DOI: 10.1103/PhysRevLett.102.256802

PACS numbers: 73.40.Gk, 68.37.Ef, 71.70.Gm, 72.10.Di

Electron tunneling is one of the central themes in condensed matter physics. It lies behind fundamental phenomena like the Josephson effect [1] and tunneling magnetoresistance [2], and provides an extremely versatile spectroscopic tool, both in tunneling junction [3,4] and STM geometries [5]. The use of inelastic electron tunneling to determine the vibration spectra of ensembles of molecules inside tunnel barriers goes back to the seminal work of Jaklevik and Lambe [3]. They observed steps in the differential conductance  $dI/dV$  curve at particular values of the bias voltages which matched the vibrational energy spectra of different molecules. This led to the notion of inelastic assisted tunneling [3,6]: an electron could tunnel across the barrier giving away its excess energy  $eV$  to create an elementary excitation. In this framework, as  $eV$  increases, new inelastic transport channels open, resulting in steps in the  $dI/dV$  curve.

With the advent of the STM, it has been possible to downscale the technique of inelastic tunneling vibrational spectroscopy to the single molecule level [7], a possibility anticipated in the early days of STM [8]. In a series of striking experiments [9–12] Heinrich *et al.* have used inelastic STM spectroscopy to probe the spin-flip excitations of a single and a few transition metal atoms in a surface by means of STM spectroscopy (STS). They have measured the single-Mn-atom Zeeman gap [9,11], the collective spin excitations of chains of up to 10 Mn atoms [10] and the spin-flip transitions within the ground state manifold of a single iron, cobalt, and Ti atom, split due to the single-atom magnetic anisotropy [11,12]. Analogously, inelastic STM spectroscopy has been used to probe the spin excitations of both Co and Fe Phthalocyanines [13,14]. Inelastic STS complements spin-polarized STS [15] which is sensitive to the average relative orientation of the magnetic moments of tip and surface ( $\vec{m}_T$  and  $\vec{m}_S$  respectively).

In contrast to the case of vibrational spectroscopy [6], the physical origin of coupling between the transport electrons and the local spins which makes SITS possible is not clear [16]. Hirjibehendin *et al.* mention two possibilities [11], exchange or dipolar coupling, although the former encompasses a variety of different mechanisms, like direct,

kinetic, etc. The coupling must account for a number of experimental observations. The height of the steps in the  $dI/dV$  scales like the sum of the squares of the matrix elements between the initial and final states of the operators  $S_a$  with  $a = x, y, z$ , the spin of the atom probed by the SITS [11]. This is related to the selection rule for the change of the spin of the local spin  $\delta S_z = \pm 1, 0$  [10,13]. Therefore, there is a relation between the inelastic current and the *spin spectral weight*  $S_{aa}(\omega)$  of the magnetic atom (s). In this Letter I show that an effective spin-assisted tunneling Hamiltonian naturally explains the relation between the inelastic current and the spin spectral weight  $S_{aa}(\omega)$  and accounts for the main experimental findings. The theory is used to analyze in detail the observed spectra of single Fe and Mn atoms and Mn chains.

The experimental system consists of an insulating thin layer deposited on a metallic surface. Magnetic atoms lie in the insulating layer and are probed by a STM. A natural model for this system would thus feature 3 types of fermion operators, tip, surface and insulating layer, plus the spin operator of the magnetic atoms. In such an approach, the current, evaluated to lowest order in the tunneling coupling, is related to the spectral function of the transport electron in the insulating layer interacting with the local spins [17]. This is different from the experimental findings described above. Thus, within the three-fermion approach the low bias steps found experimentally must arise from higher order cotunneling processes [18]. Here I adopt a simpler approach using a phenomenological Hamiltonian with two types of electrons (tip and surface), with an effective spin-flip-assisted tunneling term [19]:

$$\mathcal{H} = \mathcal{H}_{\text{tip}} + \mathcal{H}_{\text{sur}} + \mathcal{H}_S + \mathcal{H}_{\text{tun}}. \quad (1)$$

The first three terms describe the electrons in the tip ( $\mathcal{H}_{\text{tip}} = \sum_{k,\sigma} \epsilon_k a_{k\sigma}^\dagger a_{k\sigma}$ ) and in the surface ( $\mathcal{H}_{\text{sur}} = \sum_{p,\sigma} \epsilon_p b_{p\sigma}^\dagger b_{p\sigma}$ ). The Hamiltonian of the central spin(s) is the sum of the interatomic  $\mathcal{H}_{0S}(i)$  and interatomic terms  $\mathcal{H}_S = \sum_i \mathcal{H}_{0S}(i) + \sum_{i \neq j, a} j_{ab}(i, j) \hat{S}_a(i) \cdot \hat{S}_b(j)$ . The eigenenergies and eigenstates of  $\mathcal{H}_S$  are denoted by  $E_M$  and  $|M\rangle$ . Within this approach the tunneling terms read [19,20]:

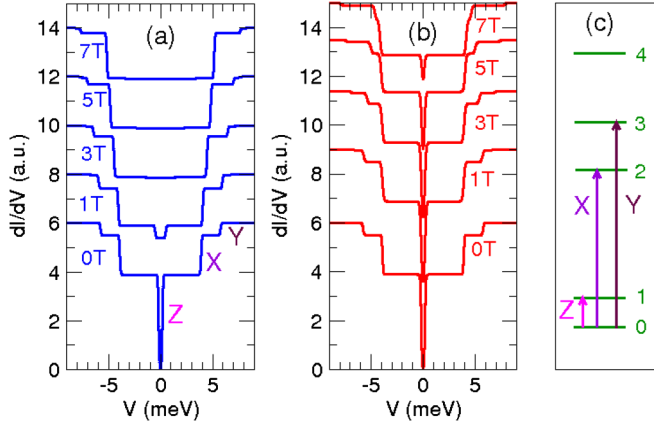


FIG. 1 (color online). (a) Differential conductance for single Fe atom with magnetic field along the  $z$  axis. (b) The same with magnetic field along the  $x$  axis. (c) Scheme of the  $B = 0$  energy levels of Eq. (8) and the tunneling induced transitions.

$$\mathcal{H}_{\text{tun}} = \sum_{\sigma\sigma'\alpha,i} T_{\alpha}(kk', i) \frac{\tau_{\sigma\sigma'}^{\alpha}}{2} \hat{S}^{\alpha}(i) (a_{k\sigma}^{\dagger} b_{k'\sigma'} + \text{H.c.}), \quad (2)$$

where  $\tau^{\alpha}$  and  $\hat{S}^{\alpha}(i)$  are the Pauli matrices and the spin operators of the atom  $i$  in the central region for  $\alpha = a = x, y, z$ , and the unit matrix for  $\alpha = 0$ . Because of the short-range nature of exchange interaction and tunneling processes from the tip in most instances there is a dominant  $T_{\alpha}(kk', i)$  for the magnetic atom  $i$  underneath the tip. Terms with  $\alpha \neq 0$  describe a Kondo-like exchange of the local spins with a conduction electron that scatters between the tip and surface. Unlike a conventional tunnel, this is a four fermion term. In the case of the Anderson model, this exchange assisted tunneling is antiferromagnetic (AFM) and arises naturally from a second-order cotunneling process [21]. The AFM nature of the coupling is supported by the observation of the Kondo effect in the case of Co adatoms [12].

Equation (2) describes both spin-assisted ( $\alpha = x, y, z$ ) and conventional tunneling  $\alpha = 0$ . To lowest order in  $\mathcal{H}_{\text{tun}}$ , the current has three contributions: (i) a central-spin independent  $T_0^2$ , (ii) crossed contributions proportional to  $T_0 T_a \vec{m}_{T,S} \cdot \langle \vec{S}(1) \rangle$ , and (iii) a spin-flip contribution  $T_a^2$  that features the spin spectral weight and is responsible of the steps in the  $dI/dV$  curves. In the case of the magnetized tip and sample the  $T_0^2$  contribution depends on  $\vec{m}_T \cdot \vec{m}_S$  which makes possible the SP-STs spectroscopy [15,22]. In this work  $\vec{m}_S = \vec{m}_T = 0$ . In the absence of atomic spin coherence, the spin-flip contribution reads [19]

$$I = \sum_M P_M \left( \sum_{p,\sigma} n_p^T \gamma_{p,M}^{T \rightarrow S} - \sum_{k,\sigma} n_k^S \gamma_{k,M}^{S \rightarrow T} \right), \quad (3)$$

where  $P_M$  is the (nonequilibrium) occupation of the  $M$  state,  $n_p^{T,S}$  is the occupation function of the tip and surface and  $\gamma$  is the tunneling rates associated to the spin-flip-assisted tunneling Hamiltonian:

$$\gamma_{p,M}^{T \rightarrow S} = \sum_{p',M',a} |\langle M | \sum_i T_a(pp', i) \hat{S}^a(i) | M' \rangle|^2 \times (1 - n_{p'}^S) \delta(\epsilon_{p'} + \epsilon_{M'} - \epsilon_p - \epsilon_M). \quad (4)$$

This expression gives the lifetime of a product state with an electron in the state  $p$  of the tip and the magnetic atom(s) in state  $M$  due to a spin-flip-assisted tunneling of the electron to the surface. Importantly, in the case of a single central spin this equation relates current to the spin matrix elements,  $|\langle M | S^a | M' \rangle|^2 \equiv |S_{M,M'}^a|^2$ , as reported in the experiments [10,11,13].

If the coupling between transport electrons and spins is rotationally invariant,  $T_a(i) = T_S(kk')\eta(i)$  is the same for  $a = x, y$ , and  $z$ . Here  $\eta(i)$  is a dimensionless number that accounts for the different tunneling probability through different atoms in the chain. The dependence of  $T_S(kk')$  on the momentum indexes can be neglected. We take  $n^T(\epsilon) = f(\epsilon)$  and  $n^S(\epsilon) = f(\epsilon + eV)$ , where  $f$  is the Fermi function. The sum over momenta leads to an integral over energies featuring the density of states of tip and surface,  $\rho_T(\epsilon)$  and  $\rho_S(\epsilon)$  which are assumed to be flat in the neighborhood of the Fermi energy. I define  $eG_S \equiv T_S^2 \rho_T(\epsilon_F) \rho_S(\epsilon_F)$ , and  $F(\epsilon, \epsilon', \omega) = [f(\epsilon)(1 - f(\epsilon' + \omega)) - f(\epsilon + \omega)(1 - f(\epsilon'))]$  so that the current reads

$$I = G_S \sum_{i,i',a=x,y,z} \int_{-\infty}^{\infty} \int_{-\infty}^{\infty} \mathcal{S}_{aa}(\epsilon - \epsilon') F(\epsilon, \epsilon', eV) d\epsilon d\epsilon', \quad (5)$$

where

$$\mathcal{S}_{aa}(\omega) \equiv \sum_{M,M'} P_M |\langle M | \mathbf{S}^a | M' \rangle|^2 \delta(\omega - \Delta_{M',M}), \quad (6)$$

where  $\mathbf{S}^a \equiv \sum_i \eta(i) S^a(i)$  and  $\Delta_{M',M} \equiv \epsilon_{M'} - \epsilon_M$ . For a single spin  $\mathbf{S}^a = S^a$ . The quantity  $\mathcal{S}_{aa}(\omega)$  is dubbed *spin spectral weight* in analogy with the dipole spectral weight [6]. After two integrations the total inelastic current is thus written as

$$I = \sum_{M,M',a,s=\pm} P_M |\langle M | \mathbf{S}^a | M' \rangle|^2 \frac{eV - s\Delta}{1 - e^{-s\beta(eV - s\Delta)}}. \quad (7)$$

Equations (5) and (7) are the magnetic analog of the vibrational inelastic tunneling spectroscopy [6] in which the dipole spectral weight of the molecular vibrations is replaced by the spin spectral weight of the magnetic atoms.

From the formal point of view, Eq. (5) is one of the main results of this Letter. It relates the inelastic current to the spin spectral weight of the magnetic atom(s) probed by the STM. Equation (5) shows that two types of spin-assisted tunneling processes contribute to the current. If we choose  $z$  as the quantization axis, the  $a = x, y$  terms involve spin exchange between the transport electron and the magnetic atom. These are the spin-flip terms. In contrast, the  $a = z$  term conserves the spin of both carrier and atom.

Now the validity of Eqs. (5) and (7) and thereby that of the spin-assisted tunneling term (2) is verified by comparing their predictions with the experimental results. To do

so, spin model Hamiltonians  $\mathcal{H}_S$  and their eigenstates are needed. For simplicity I approximate  $P_M$  by an equilibrium distribution, independent of voltage. The case of tunneling through a single Fe atom in  $\text{Cu}_2\text{N-Cu}$  system [11] is considered first. Following that reference, the standard single-spin Hamiltonian reads

$$\mathcal{H}_S = D\hat{S}_z^2 + E(\hat{S}_x^2 - \hat{S}_y^2) + g\mu_B\vec{B} \cdot \vec{S} \quad (8)$$

with  $S = 2$  adequate for  $\text{Fe}^{2+}$  and  $D = -1.55$  meV and  $E = 0.35$  meV [11]. The ground (first excited) state is made mainly (only) with  $M_z = \pm 2$ . The  $dI/dV$  curves obtained from Eq. (7) and the exact solution of Hamiltonian (8) for different intensities and orientations of the applied magnetic field, evaluated for  $k_B T = 0.5$  K, are shown in Figs. 1(a) and 1(b). The a (b) panel corresponds to field parallel to  $z$  ( $x$ ). At zero field the  $dI/dV$  curves shows three steps corresponding to the excitations to the first, second and third excited states. The transition to the fourth state is forbidden ( $\sum_{a=x,y,z} |\langle 0|S_a|4\rangle|^2 = 0$ ). The prominent  $0 \rightarrow 1$  transition comes from the spin-conserving channel  $a = z$ , where as the  $0 \rightarrow 2$  and  $0 \rightarrow 3$  transitions come from the spin-flip channels  $a = y$  and  $a = x$ , respectively (see Fig. 1(c)). The evolution of the  $dI/dV$  curves as a function of the intensity and orientation of  $\vec{B}$  give good account of the main observed experimental features [11].

The theory also accounts for more complicated experimental situations where electrons tunnel through one magnetic atom which is exchanged coupled to others. This is the case of linear chains of  $\mathcal{N}$  Mn atoms deposited on a

$\text{Cu}_2\text{N-Cu}$  surface,  $\mathcal{N}$  going from 1 to 10. The  $dI/dV$  curves of the chains showed marked even-odd  $\mathcal{N}$  effects accounted for by a first-neighbor AFM Heisenberg coupling [10]. However, this model can not account for the small bias dip observed for odd  $\mathcal{N}$  chains, the zero field splitting of the first step in the  $\mathcal{N} = 2$  chain and the redshift of the step at 17 meV in the  $\mathcal{N} = 3$  chain. Here I extend the first-neighbor Heisenberg model without single-ion terms used by Hirjibehedin [10] *et al.* in two ways. First, the single-ion magnetic anisotropy, found by Hirjibehedin *et al.* for Mn on  $\text{Cu}_2\text{N}$  [11], is included in the Hamiltonian of the chain. Second, in the case of the trimer, the second-neighbor coupling must be included to account for the experimental data. Thus, the model reads

$$\mathcal{H}_S = \sum_i \mathcal{H}_S(i) + \sum_{i,j} J_{ij} \vec{S}(i) \cdot \vec{S}(j), \quad (9)$$

where the sum in the last term runs over  $i \neq j$ . This Hamiltonian is diagonalized numerically. Figure 2(a) shows a summary of the  $dI/dV$  curves for monomers, dimers, trimers, and tetramers in good agreement with experiment [10]. According to experiments [10] the single-ion anisotropy term for  $\text{Mn}^{2+}$  on top of Cu is  $D = -0.039$  meV. It is possible to account for the fine structure of the dimer and the trimer keeping the same value for all the atoms in the chain. The values of the first-neighbor exchange coupling constants are at least 10 times larger and positive (AFM). Thus, to a very good approximation we can label the eigenstates of (9) with  $S$  and  $S_z$ , total spin  $S$  and a projection along the  $z$  axis, taken perpendicular to the surface in this case.

The ground state and first excited states of the dimer have spin  $S = 0$  and  $S = 1$ , respectively. Both in this set of experiments [10] and in the calculations below, a magnetic field is applied in the plane, at 55 degrees of the  $x$  axis in which the dimer lies, splitting the states of the  $S = 1$  triplet. Three steps are resolved at finite field, corresponding to the three transitions  $S = 0 \rightarrow (S = 1, S_z = \pm 1, 0)$ . At large fields the observed [10] energies satisfy  $\Delta(S_z, B) = \Delta_0(S_z) + g\mu_B S_z B$ . Importantly,  $\Delta_0(S_z = \pm 1) = 5.83 \pm 0.05$  meV, different from  $\Delta_0(S_z = 0) = 5.96 \pm 0.05$  meV,  $g = 2.1$ . This zero field splitting *cannot* be accounted for by the Heisenberg model, for which the zero field excitation energy is independent of  $S_z$  and equal to  $\Delta_{1,0} = J$ . In Fig. 2(b) I show the evolution of the  $dI/dV$  curves and the excitation energies  $\Delta_{1,0}(S_z)$  as a function of  $B$ , using Hamiltonian (9). For large values of  $B$ , the excitation energies can be fitted with straight lines. Extrapolation of the high field simulation to zero field yield  $\Delta_0(S_z = +1) = 5.83$  meV,  $\Delta_0(S_z = -1) = 5.86$  meV and  $\Delta_0(S_z = 0) = 5.94$ , in agreement with the experiment within the experimental error bar. Notice, however, that at low field, for which there is no published data, the curves are no longer linear due to the competition between the applied field and magnetic anisotropy [Fig. 2(c)]. The only free parameter in this calculation is  $J = 5.88$  meV.

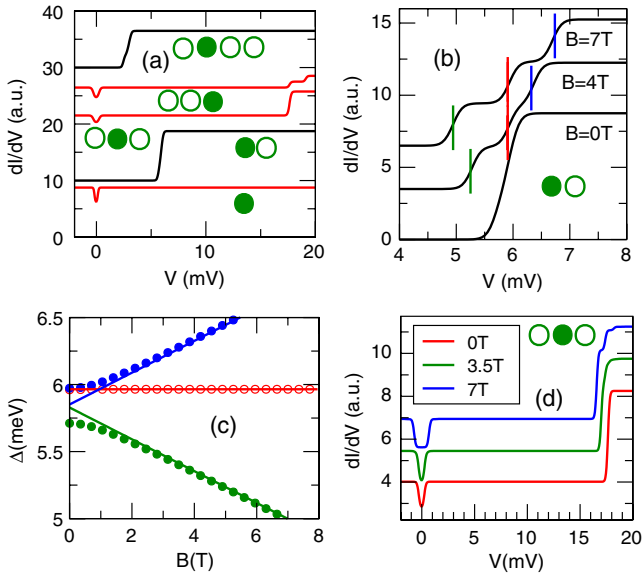


FIG. 2 (color online). (a)  $dI/dV$  for  $B = 0$ ,  $k_B T = 0.6$  K for chains of  $\mathcal{N}$  Mn atoms,  $\mathcal{N} = 1, 2, 3, 4$ . Solid circles represent the atom underneath the tip. (b) Evolution of the  $dI/dV$  for  $\mathcal{N} = 2$  for 3 values of  $B$ . (c) Evolution of the corresponding excitations. (d) Evolution of the  $dI/dV$  for  $\mathcal{N} = 3$  for 3 values of  $B$ . In all the cases  $\vec{B}$  lies in plane,  $55^\circ$  from the chain.

The experimental data for the trimer shows a first step below 1 meV, and a second step at 17.5 meV. The position of the second step shifts towards low energy as a magnetic field is applied. Neither of these two results can be accounted for by a first-neighbor AFM Heisenberg model for which the ground state has  $S = 5/2$  and the first two excited manifolds have  $S = 3/2$  and  $S = 7/2$  with excitation energies  $\Delta_{3/2,5/2} = 2.5J$  and  $\Delta_{7/2,5/2} = 2.5J$ . Taking  $J = 5.88$  meV from the dimer,  $\Delta_{5/2,3/2} = 14.7$  meV and  $\Delta_{5/2,7/2} = 20.58$  meV. The addition of single-ion anisotropy splits the 6 states of the  $S = 5/2$  manifold in 3 doublets, according to  $E = 1.65D_3S_z^2$ , with  $D_3 = 1.65D$ . Since  $D_3 < 0$ , the trimer behaves like a  $S = 5/2$  nanomagnet with spin  $S_z = \pm 5/2$  as the ground state. The anisotropy barrier is given by  $6D_3 \approx 4$  K. Internal transitions within the  $S_z = \pm 5/2$  ground state and the  $S_z = \pm 3/2$  excited states of the  $S = 5/2$  manifold account for the low bias dip and its evolution as a function of the applied field  $B$  [see Fig. 2(d)].

In order to account for the 17.5 meV structure it is not enough to invoke a reduction of the first-neighbor coupling  $J$  due to small changes in the crystal environment, because the observed redshift of the 17.5 meV structure can only be possible for a transition from the  $S = 5/2$  ground to the  $S = 7/2$  state. Thus, it is necessary to go beyond the first neighbor Heisenberg model. A natural option is to consider second neighbor coupling  $J_2$ , that could arise from RKKY coupling, and could either ferromagnetic (FM) or AFM, and is presumably smaller than  $J$ . Using a FM  $J_{13}$ ,  $\Delta_{7/2,5/2}$  turns out to be independent of  $J_{13}$  whereas  $\Delta_{3/2,5/2} = 3.5J + 5|J_{13}|$ . Thus, when  $-5J_{13} > J$  the transition to the  $7/2$  manifold becomes the first excited state (outside the  $S = 5/2$  anisotropy split manifold). Thus, the position of the step and its redshift can be modeled taking  $J = J_{1,2} = J_{2,3} = 5$  meV and  $J_2 \equiv J_{1,3} = -1.3$  meV [Fig. 2(d)]. Additionally, the amplitude of the  $dI/dV$  step associated to the  $\Delta_{7/2,5/2}$  transition is always finite, regardless of which atom is below the tip, in contrast with the step associated to  $\Delta_{3/2,5/2}$ , which is forbidden for the central atom [Fig. 2(a)]. Thus, the spin-assisted tunneling spectroscopy can be used to map the wave function of the spin excitations.

Finally, I consider how the second-neighbor coupling affects the tetramer, which was properly described with the simpler  $J_2 = 0$  model [10]. The AFM  $J$  coupling together with a weak FM  $J_2$  yield a ground state with  $S = 0$ . The first excited state has  $S = 1$  and energy approximately given by  $\Delta_{5/2,3/2} = 0.47J + 0.43|J_2|$ , for  $J \gg -J_2$  and  $J_2 < 0$ . Inspection of the experimental data [10] yields an approximate excitation energy of 2.4 meV. Taking the values for  $J$  and  $J_2$  from the trimer  $\Delta_{5/2,3/2} = 2.56$  meV. Thus, second-neighbor coupling is necessary to describe the trimer and compatible with the observations of the tetramer.

In conclusion, I show that the spin-assisted tunneling mechanism [19,21] that couples electrons in the tip and the

surface to the local spin (2) accounts for the single-spin inelastic tunneling spectroscopy experiments [9–14]. This mechanism naturally leads to an expression for the current that involves the spin spectral weight  $S_{aa}(\omega)$  of the magnetic atom below the tip and to the spin selection rules observed experimentally [10,13]. Single-ion anisotropy, AFM first-neighbor, and FM second-neighbor coupling are necessary to model the spectra of Mn chains on  $\text{Cu}_2\text{N}$ . The Mn trimer is portrayed as a nanomagnet with spin  $S = 5/2$ , ground state  $S_z = \pm 5/2$  and anisotropy barrier of 4 K.

I acknowledge fruitful discussions with R. Aguado, J. J. Palacios, F. Delgado, C. Untiedt, and C. Hirjibehedin. This work has been financially supported by MEC-Spain (Grant MAT07) and by Consolider CSD2007-0010.

*Note added.*—Recently, other work with related results has been posted [23].

- 
- [1] B. D. Josephson, Rev. Mod. Phys. **36**, 216 (1964).
  - [2] M. Julière, Phys. Lett. A **54**, 225 (1975); J. S. Moodera, L. R. Kinder, T. M. Wong, and R. Meservey, Phys. Rev. Lett. **74**, 3273 (1995).
  - [3] R. C. Jaklevic and J. Lambe, Phys. Rev. Lett. **17**, 1139 (1966).
  - [4] P. M. Tedrow and R. Meservey, Phys. Rev. B **7**, 318 (1973).
  - [5] G. Binnig and H. Rohrer, Rev. Mod. Phys. **59**, 615 (1987).
  - [6] D. J. Scalapino and S. M. Marcus, Phys. Rev. Lett. **18**, 459 (1967).
  - [7] B. C. Stipe, M. A. Rezaei, and W. Ho, Science **280**, 1732 (1998).
  - [8] G. Binnig, N. Garcia, and H. Rohrer, Phys. Rev. B **32**, 1336 (1985).
  - [9] A. J. Heinrich, J. A. Gupta, C. P. Lutz, and D. M. Eigler, Science **306**, 466 (2004).
  - [10] C. F. Hirjibehedin, C. P. Lutz, and A. J. Heinrich, Science **312**, 1021 (2006).
  - [11] C. Hirjibehedin *et al.*, Science **317**, 1199 (2007).
  - [12] A. F. Otte *et al.*, Nature Phys. **4**, 847 (2008).
  - [13] Xi. Chen *et al.*, Phys. Rev. Lett. **101**, 197208 (2008).
  - [14] N. Tsukahara *et al.*, Phys. Rev. Lett. **102**, 167203 (2009).
  - [15] F. Meier *et al.*, Science **320**, 82 (2008).
  - [16] M. Persson, arXiv:0811.2511; N. Lorente and J. P. Gauyacq, arXiv:0904.4327.
  - [17] J. Fernández-Rossier and R. Aguado, Phys. Rev. Lett. **98**, 106805 (2007).
  - [18] F. Elste and C. Timm, Phys. Rev. B **75**, 195341 (2007).
  - [19] J. A. Applebaum, Phys. Rev. **154**, 633 (1967).
  - [20] Z. Nussinov, M. F. Crommie, and A. V. Balatsky, Phys. Rev. B **68**, 085402 (2003); G. H. Kim and T. S. Kim, Phys. Rev. Lett. **92**, 137203 (2004).
  - [21] P. W. Anderson, Phys. Rev. Lett. **17**, 95 (1966).
  - [22] D. Wortmann, S. Heinze, Ph. Kurz, G. Bihlmayer, and S. Blügel, Phys. Rev. Lett. **86**, 4132 (2001).
  - [23] J. Fransson, O. Eriksson, and A. V. Balatsky, arXiv:0812.4956; A. N. Rudenko *et al.*, Phys. Rev. B **79**, 144418 (2009).